

Обзор ArXiv:astro-ph,
13-17 марта 2017 года

От Сильченко О.К.

Astro-ph: 1703.05491

FALLING OUTER ROTATION CURVES OF STAR-FORMING GALAXIES AT $0.6 \lesssim Z \lesssim 2.6$ PROBED WITH KMOS^{3D}
AND SINS/ZC-SINF

PHILIPP LANG^{1,2}, NATASCHA M. FÖRSTER SCHREIBER¹, REINHARD GENZEL^{1,3,4}, STIJN WUYTS⁵, EMILY WISNOSKI¹, ALESSANDRA BEIFIORI^{1,6},
SIRIO BELLÌ¹, RALF BENDER^{1,6}, GABE BRAMMER⁷, ANDREAS BURKERT^{1,6}, JEFFREY CHAN¹, RIC DAVIES¹, MATTEO FOSSATI^{1,6}, AUDREY
GALAMETZ¹, SANDESH K. KULKARNI¹, DIETER LUTZ¹, J. TREVOR MENDEL¹, IVELINA G. MOMCHEVA⁷, THORSTEN NAAAB⁸, ERICA J. NELSON¹,
ROBERTO P. SAGLIA^{1,6}, STELLA SEITZ⁶, SANDRO TACCHELLA¹⁰, LINDA J. TACCONI¹, KEN-ICHI TADAKI¹, HANNAH ÜBLER¹, PIETER G. VAN
DOKKUM⁹, DAVID J. WILMAN^{1,6}

¹Max-Planck-Institut für extraterrestrische Physik, Giessenbachstrasse, D-85748 Garching, Germany

²Max-Planck-Institut für Astronomie, Königstuhl 17, D-69117 Heidelberg, Germany

³Department of Physics, Le Conte Hall, University of California, Berkeley, CA 94720, USA

⁴Department of Astronomy, New Campbell Hall, University of California, Berkeley, CA 94720, USA

⁵Department of Physics, University of Bath, Claverton Down, Bath, BA2 7AY, UK

⁶Universitäts-Sternwarte München, Scheinerstr. 1, München, D-81679, Germany

⁷Space Telescope Science Institute, 3700 San Martin Drive, Baltimore, MD 21218, USA

⁸Max-Planck-Institut für Astrophysik, Karl Schwarzschildstr. 1, D-85748 Garching, Germany

⁹Astronomy Department, Yale University, New Haven, CT 06511, USA

¹⁰Institute of Astronomy, Department of Physics, Eidgenössische Technische Hochschule, ETH Zürich, CH-8093, Switzerland

101 галактика между $z=0.6$ и $z=2.6$ – просуммировали!

Table 1. Median properties of the stacking sample.

Property	Median
z	1.52
$\log(M_*[M_\odot])$	10.61
$\log(M_{\text{baryonic}} = M_* + M_{\text{gas}}^a)[M_\odot]$	10.87
$SFR [M_\odot/\text{yr}]$	41.9
$sSFR [\text{Gyr}^{-1}]$	1.20
$R_e^b [\text{kpc}]$	4.6
n^b	1.1

^aGas mass estimate based on empirical scaling relations.

^bIntrinsic effective radius along the major axis and Sérsic index derived from H -band Sérsic fits.

... Вписали в кривую вращения ионизованного газа модель экспоненциального диска

the noise cube associated with each data cube. Once we have constructed a rotation curve for each galaxy, we determine its observed amplitude and extent by fitting a Freeman exponential disk model of the form:

$$v_{\text{disk}}(r) = \frac{r}{r_d} \sqrt{\pi G \Sigma_0 r_d [I_0 K_0 - I_1 K_1]}, \quad (1)$$

where r_d is the radial scale-length of the exponential disk, corresponding to $r_d = R_e/1.68$. Σ_0 is the central mass surface density of the disk, and I_n and K_n denote the modified Bessel functions of the first and second kind (Freeman 1970). In the fitting, we leave r_d and Σ_0 as free parameters. Before fitting, the Freeman disk model is convolved with a 1D Gaussian of FWHM corresponding to the PSF associated with each galaxy. After the fit has converged, we determine the maximum observed velocity (V_{max}) and the radius of the peak (R_{turn}) from the model. In the right panels of Figure 2, rotation curves of two examples are shown together with the respective fit.

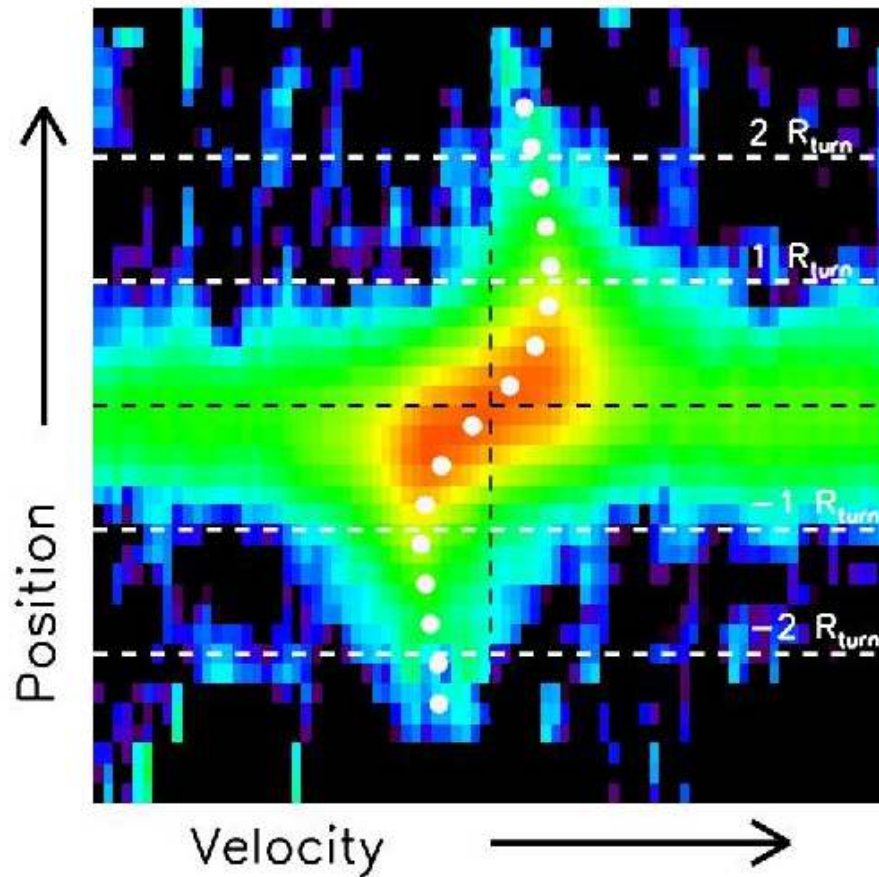


Figure 3. Final stacked pv diagram shown in logarithmic color scaling. The zero positions in velocity and radius are marked as black lines, and the radial position of $1R_{\text{turn}}$ and $2R_{\text{turn}}$ are marked as white dashed horizontal lines. The white symbols

Результаты

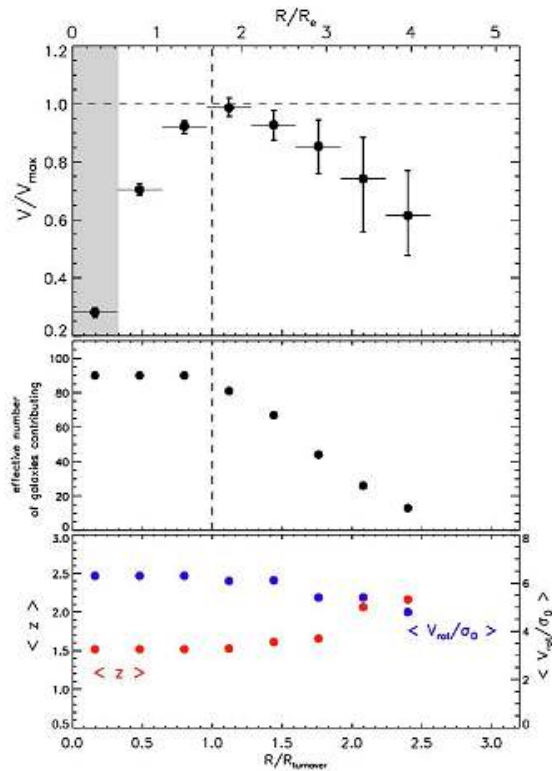
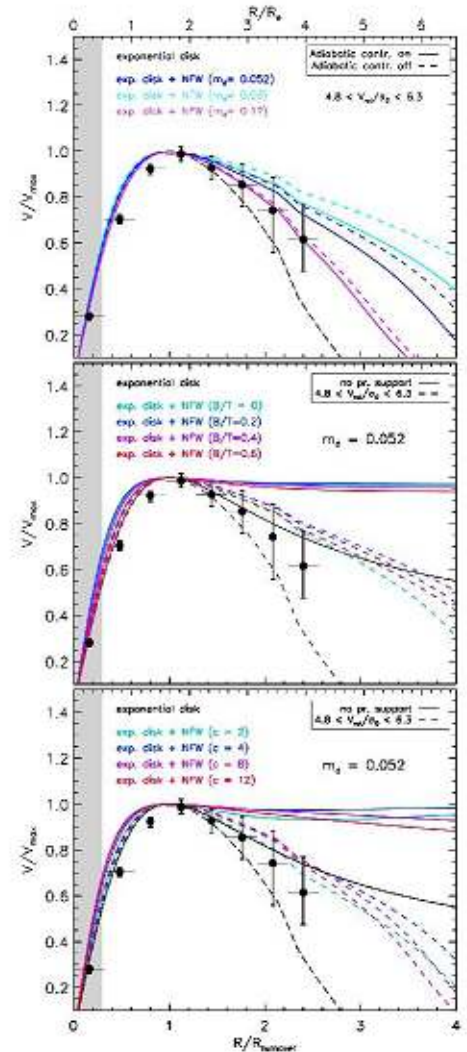
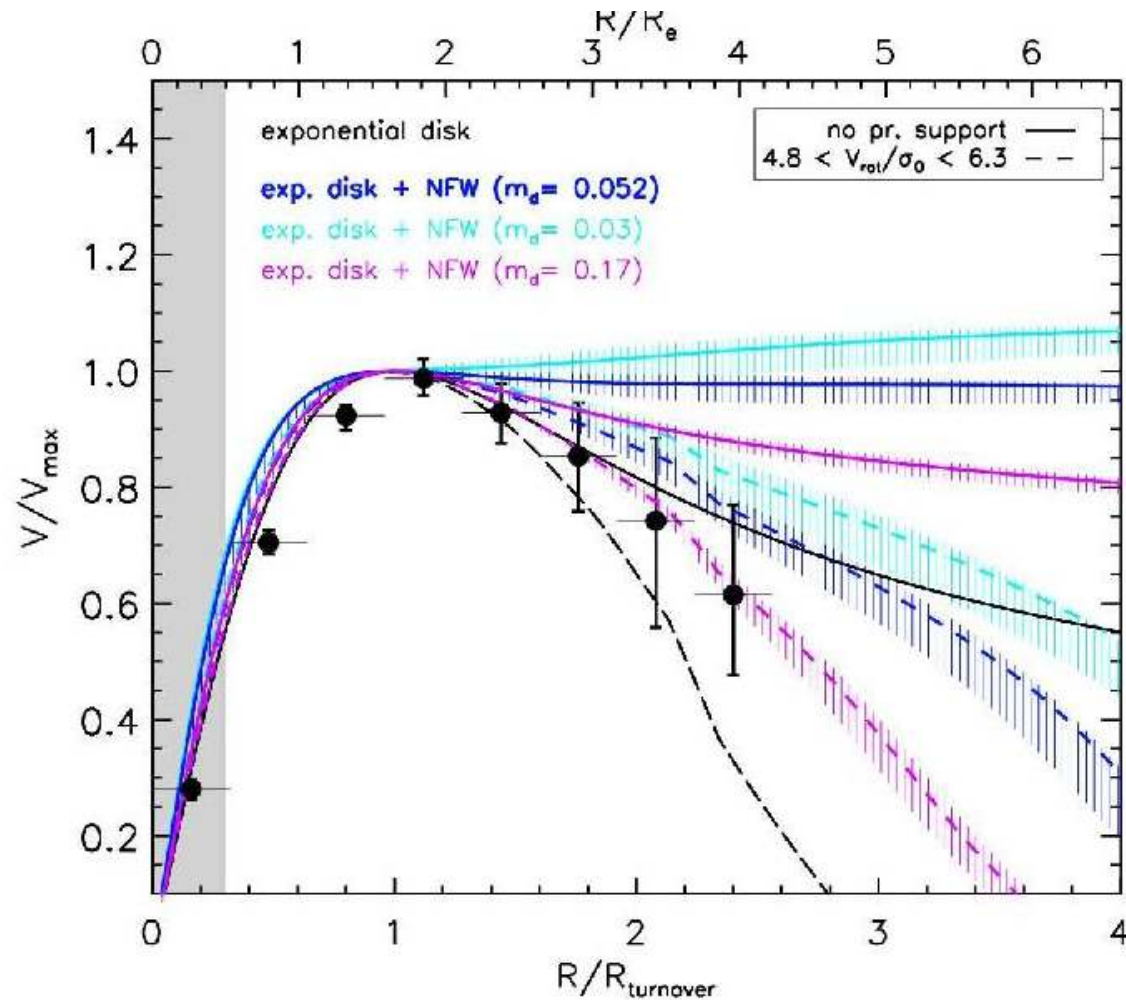


Figure 5. Top: Stacked rotation curve (black dots) plotted in units of normalized velocity (V/V_{max}), normalized radius (R/R_{turn}), and intrinsic effective radius (R/R_c). The error bars are derived from bootstrapping and include both sample variance as well as RMS noise in the spectra. The shaded area marks the half-light beam size of the average PSF observed for our sample. Middle: Effective number of galaxies contributing to the stack, accounting for masking out noisy pixels in the pv diagrams. The decrease in the number of contributing galaxies with increasing radius is driven by FOV limitations. Bottom: Median redshift and V_{rot}/σ_0 of contributing galaxies for a given radial bin.



Главный результат – темное гало НЕ чувствуется (но подразумевается...)



Astro-ph: 1703.04310 (Nature!)

Strongly baryon-dominated disk galaxies at the peak of galaxy formation ten billion years ago[†]

R.Genzel^{1,2*}, N.M. Förster Schreiber^{1*}, H.Übler¹, P.Lang¹, T.Naab³, R.Bender^{4,1}, L.J.Tacconi¹, E.Wisnioski¹, S.Wuyts^{1,5}, T.Alexander⁶, A. Beifiori^{4,1}, S.Belli¹, G. Brammer⁷, A.Burkert^{3,1}, C.M.Carollo⁸, J. Chan¹, R.Davies¹, M. Fossati^{1,4}, A.Galametz^{1,4}, S.Genel⁹, O.Gerhard¹, D.Lutz¹, J.T. Mendel^{1,4}, I.Momcheva¹⁰, E.J.Nelson^{1,10}, A.Renzini¹¹, R.Saglia^{1,4}, A.Stemberg¹², S.Tacchella⁸, K.Tadaki¹ & D.Wilman^{4,1}

¹*Max-Planck-Institut für extraterrestrische Physik (MPE), Giessenbachstr.1, 85748 Garching, Germany*
(genzel@mpe.mpg.de, forster@mpe.mpg.de)

²*Departments of Physics and Astronomy, University of California, 94720 Berkeley, USA*

³*Max-Planck Institute for Astrophysics, Karl Schwarzschildstrasse 1, D-85748 Garching, Germany*

⁴*Universitäts-Sternwarte Ludwig-Maximilians-Universität (USM), Scheinerstr. 1, München, D-81679, Germany*

⁵*Department of Physics, University of Bath, Claverton Down, Bath, BA2 7AY, United Kingdom*

⁶*Dept of Particle Physics & Astrophysics, Faculty of Physics, The Weizmann Institute of Science, POB 26, Rehovot 76100, Israel*

⁷*Space Telescope Science Institute, Baltimore, MD 21218, USA*

⁸*Institute of Astronomy, Department of Physics, Eidgenössische Technische Hochschule, ETH Zürich, CH-8093, Switzerland*

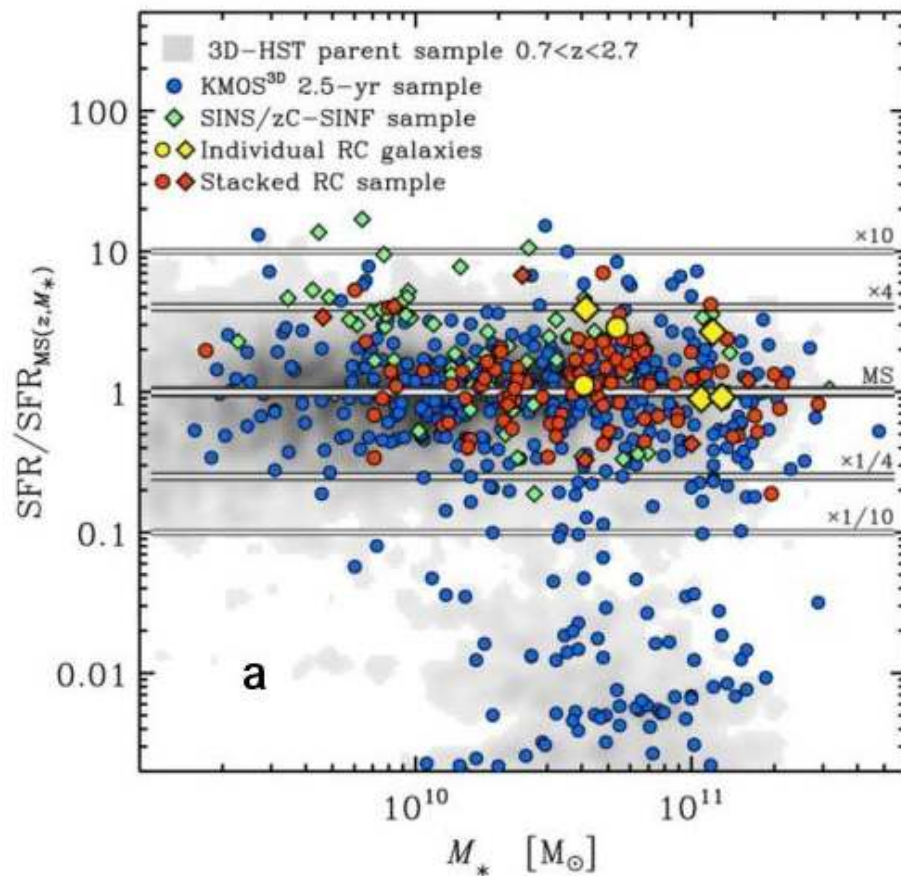
⁹*Center for Computational Astrophysics, 160 Fifth Avenue, New York, NY 10010, USA*

¹⁰*Department of Astronomy, Yale University, 260 Whitney Avenue, New Haven, CT 06511, USA*

¹¹*Osservatorio Astronomico di Padova, Vicolo dell'Osservatorio 5, Padova, I-35122, Italy*

¹²*School of Physics and Astronomy, Tel Aviv University, Tel Aviv 69978, Israel*

Выборка



Измерения

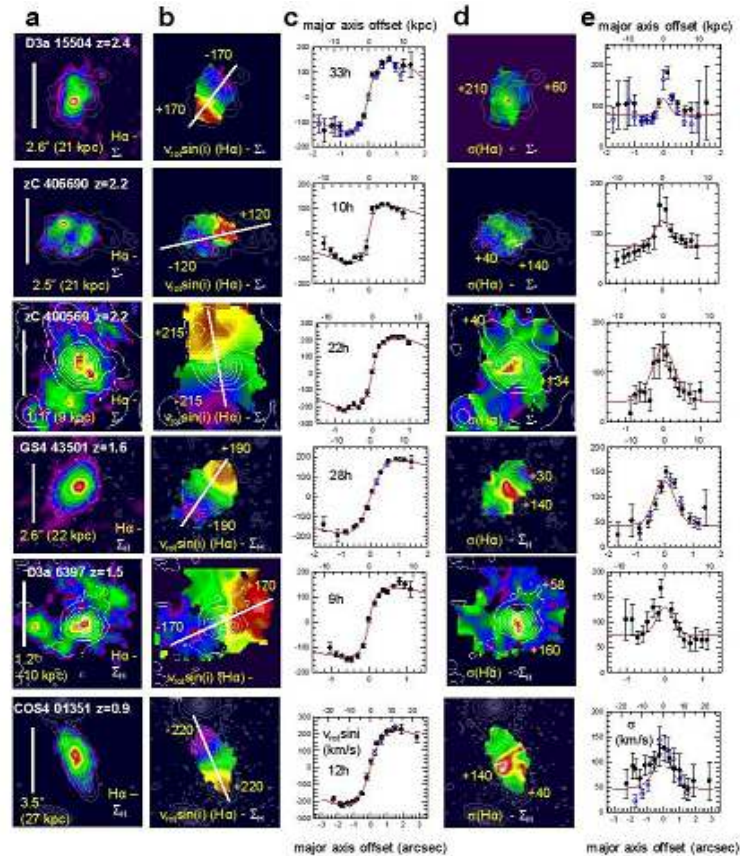


Figure 1. $H\alpha$ gas dynamics from KMOS and SINFONI in six massive star-forming galaxies. The galaxies have redshifts between $z=0.9$ and 2.4 . KMOS provides seeing-limited data (FWHM $\sim 0.6''$), and SINFONI allows both seeing-limited, and adaptive optics assisted observations (FWHM $\sim 0.2''$). For each galaxy column (a) shows the distribution of the integrated $H\alpha$ line surface brightness (with a linear colour scale), superposed on white contours of the stellar surface density (Σ_*) or the H-band continuum surface brightness (Σ_{H1}) (square root scaling). The vertical white bar denotes the

01351 and GS4 53501 we show both SINFONI (black filled circles) and KMOS (open blue circles) data sets, for D3a 15504 we show SINFONI data sets at $0.2''$ (black) and $0.5''$ (blue) resolution. Red continuous lines denote the best-fit dynamical model, constructed from a combination of a central compact bulge, an exponential disk and an NFW halo without adiabatic contraction, with a concentration of $c=4$ at $z=2$ and $c=6.5$ at $z=1$. For the modelling of the disk rotation, we also take into account the asymmetric drift correction inferred from the velocity dispersion curves ((d)-(e)¹⁴). Columns (d) and (e)

Еще измерения

Table 1. Physical Parameters of Observed Star-Forming Galaxies

	COS4 01351	D3a 6397	GS4 43501	zC 406690	zC 400569	D3a 15504
redshift	0.854	1.500	1.613	2.196	2.242	2.383
kpc/arcsec	7.68	8.46	8.47	8.26	8.23	8.14
Priors:						
M_* ($10^{11} M_\odot$)	0.54±0.16	1.2±0.37	0.41±0.12	0.42±0.12	1.2±0.37	1.1±0.34
$M_{\text{baryon}}(\text{gas+stars})$ ($10^{11} M_\odot$)	0.9±0.5	2.3±1.1	0.75±0.37	1.4±0.7	2.5±1.2	2.0±1.0
H-band $R_{1/2}$ (kpc)	8.6±1.3	5.9±0.8	4.9±0.7	5.5±1	4±2	6.3±1
inclination ($^\circ$)	75±5	30±5	62±5	25±12	45±10	34±5
dark matter concentration parameter c	6.8	5	5	4	4	4
Fit parameters:						
$v_c(R_{1/2})$ (km/s) ^a	276	310	257	301	364	299
$R_{1/2}(n=1)$ (kpc)	7.3	7.4	4.9	5.5	3.3	6
σ_0 (km/s)	39	73	39	74	34	76
$M_{\text{baryon}}(\text{gas+stars, including bulge})$ ($10^{11} M_\odot$)	1.7	2.3	1.0	1.7	1.7	2.1
$M_{\text{bulge}}/M_{\text{baryon}}$	0.2	0.35	0.4	0.6	0.37	0.15
$f_{DM}(R_{1/2})=(v_{DM}/v_c)^2 _{R=R_{1/2}}$ ^b	0.21 (±0.1)	0.17 (<0.38)	0.19 (±0.09)	0.0 (<0.08)	0.0 (<0.07)	0.12 (<0.26)

^a Total circular velocity at the half-light radius (rest-frame optical) $R_{1/2}$, including bulge, exponential disk ($n=1$) and dark matter, and corrected for asymmetric drift: $v_c(R)^2=v_{\text{rot}}(R)^2+3.36 \sigma_0^2 \times (R/R_{1/2})|_{n=1}$.

^b Ratio of dark matter to total mass at the half-light radius of the optical light, $f_{DM}(R_{1/2})=(v_{DM}/v_c)^2|_{R=R_{1/2}}$, with numbers in the parentheses giving the ± 2 rms ($\delta\chi^2=4$, ~95% probability) uncertainties, or upper limits. We use an NFW halo of concentration parameter c, and no adiabatic contraction.

Главный результат: отсутствие темной материи – признак раннего типа галактики?

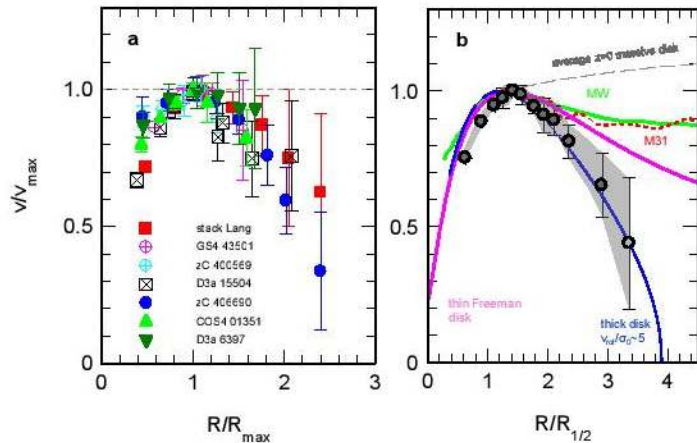


Figure 2. Normalized rotation curves. (a): The various symbols denote the folded and binned rotation curve data for the six galaxies in Figure 1, combined with the stacked rotation curve of 97 $z=0.6-2.6$ star-forming galaxies¹⁸ (Methods). For all rotation curves we averaged data points located symmetrically on either side of the dynamical centres, and plot the rotation velocities and radii normalized to their maximum values. Error bars are ± 1 rms. (b): The black data points

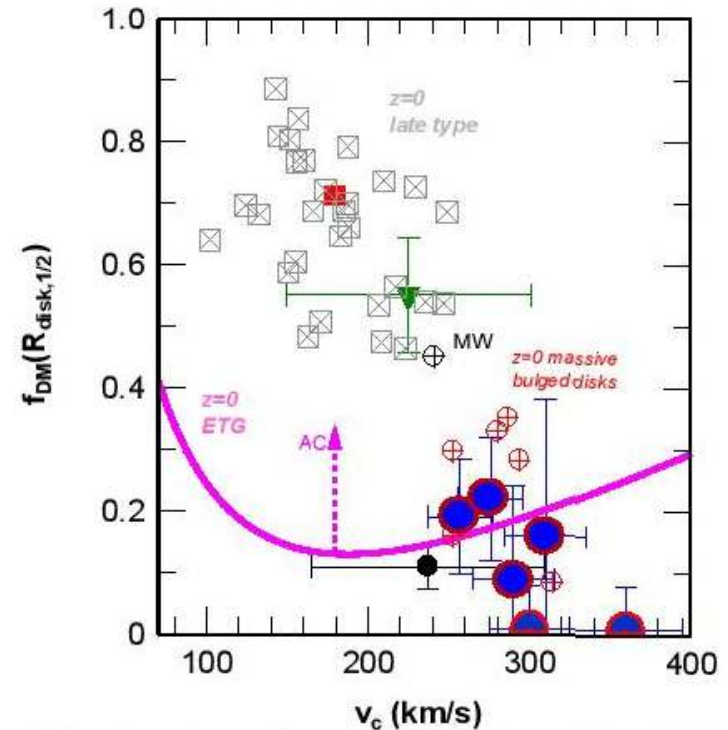


Figure 3. Dark matter fractions. Dark matter fractions from different methods are listed as a function of the circular velocity of the disk, at the half mass/light radius of the disk, for galaxies in the current Universe and ~ 10 Gyr ago. The large blue circles with red outlines indicate the dark matter fractions derived from the outer-disk rotation curves of the six high- z disks presented in this paper (Table 1), along with the ± 2 rms

Astro-ph: 1703.04321

THE EVOLUTION OF THE TULLY-FISHER RELATION BETWEEN $Z \sim 2.3$ AND $Z \sim 0.9$ WITH KMOS^{3D}

H. ÜBLER¹, N. M. FÖRSTER SCHREIBER¹, R. GENZEL^{1,2}, E. WISNIOSKI¹, S. WUYTS³, P. LANG^{1,4}, T. NAAB⁵,
D. J. WILMAN^{6,1}, M. FOSSATI^{6,1}, J. T. MENDEL^{1,6}, A. BEIFIORI^{6,1}, S. BELLI¹, R. BENDER^{6,1}, G. B. BRAMMER⁷,
A. BURKERT^{6,1}, J. CHAN^{6,1}, R. DAVIES¹, M. FABRICIUS¹, A. GALAMETZ^{1,6}, D. LUTZ¹, I. G. MOMCHEVA⁷, E. J. NELSON¹,
R. P. SAGLIA^{1,6}, S. SEITZ^{6,1}, L. J. TACCONI¹, K. TADAKI¹, P. G. VAN DOKKUM⁸

¹Max-Planck-Institut für extraterrestrische Physik, Giessenbachstr. 1, D-85737 Garching, Germany (hannah@mpe.mpg.de)

²Departments of Physics and Astronomy, University of California, Berkeley, CA 94720, USA

³Department of Physics, University of Bath, Claverton Down, Bath, BA2 7AY, United Kingdom

⁴Max-Planck-Institut für Astronomie, Königstuhl 17, D-69117 Heidelberg, Germany

⁵Max-Planck-Institut für Astrophysik, Karl Schwarzschildstr. 1, D-85737 Garching, Germany

⁶Universitäts-Sternwarte Ludwig-Maximilians-Universität München, Scheinerstr. 1, D-81679 München, Germany

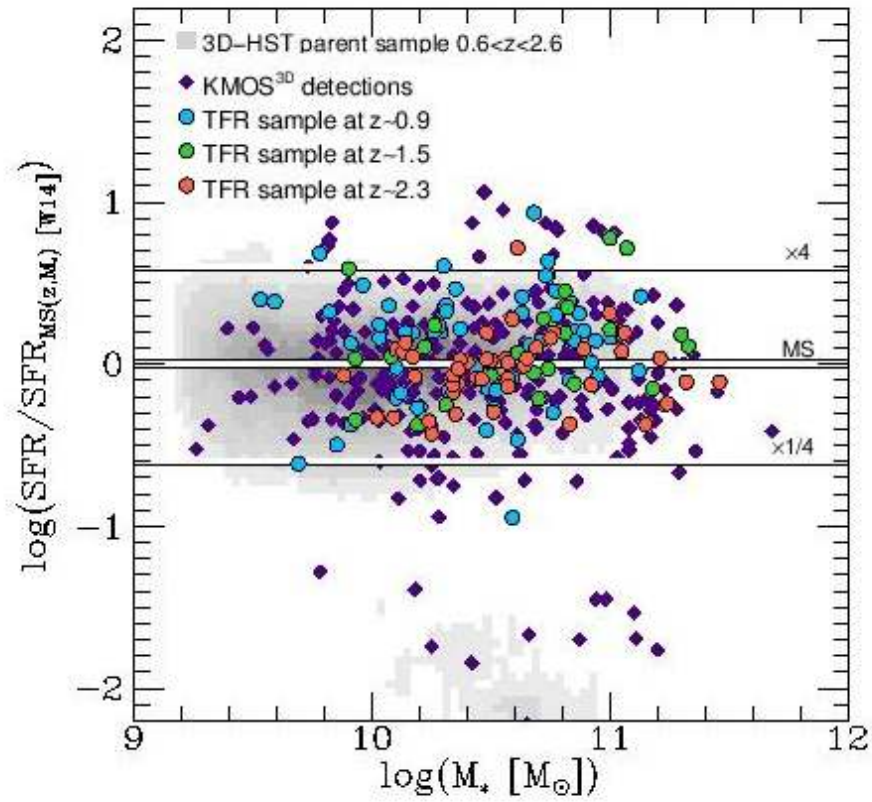
⁷Space Telescope Science Institute, 3700 San Martin Drive, Baltimore, MD 21218, USA

⁸Department of Astronomy, Yale University, New Haven, CT 06511, USA

ABSTRACT

We investigate the stellar mass and baryonic mass Tully-Fisher relations (TFRs) of massive star-forming disk galaxies at redshift $z \sim 2.3$ and $z \sim 0.9$ as part of the KMOS^{3D} integral field spectroscopy

Выборка



Выборка

Table 1. Median physical properties of our TFR subsamples at $z \sim 0.9$ (*YJ*), $z \sim 1.5$ (*H*), and $z \sim 2.3$ (*K*), together with the associated central 68th percentile ranges in brackets.

	$z \sim 0.9$ (65 galaxies)	$z \sim 1.5$ (24 galaxies)	$z \sim 2.3$ (46 galaxies)
$\log(M_* [M_\odot])$	10.49 [10.03; 10.83]	10.72 [10.08; 11.07]	10.51 [10.18; 11.00]
$\log(M_{\text{bar}} [M_\odot])$	10.62 [10.29; 10.98]	10.97 [10.42; 11.31]	10.89 [10.59; 11.33]
SFR [M_\odot/yr]	21.1 [7.1; 39.6]	53.4 [15.5; 134.5]	72.9 [38.9; 179.1]
$\log(\Delta \text{MS})^a$	0.20 [-0.21; 0.42]	0.10 [-0.21; 0.45]	-0.01 [-0.29; 0.13]
R_e^{5000} [kpc]	4.8 [3.0; 7.6]	4.9 [3.0; 7.0]	4.0 [2.5; 5.2]
$\log(\Delta \text{M-R})^b$	-0.02 [-0.17; 0.16]	0.08 [-0.10; 0.17]	0.06 [-0.14; 0.17]
n_S	1.3 [0.8; 3.1]	0.9 [0.4; 2.2]	1.0 [0.4; 1.6]
B/T^c	0.11 [0.00; 0.39]	0.00 [0.00; 0.23]	0.10 [0.00; 0.25]
$v_{\text{rot,max}}$ [km/s]	233 [141; 302]	245 [164; 337]	239 [160; 284]
σ_0 [km/s]	30 [9; 52]	47 [29; 59]	49 [32; 68]
$v_{\text{rot,max}}/\sigma_0$	6.7 [3.2; 25.3]	5.5 [3.4; 65.6]	4.3 [3.4; 9.1]
$v_{\text{circ,max}}$ [km/s]	239 [167; 314]	263 [181; 348]	260 [175; 315]

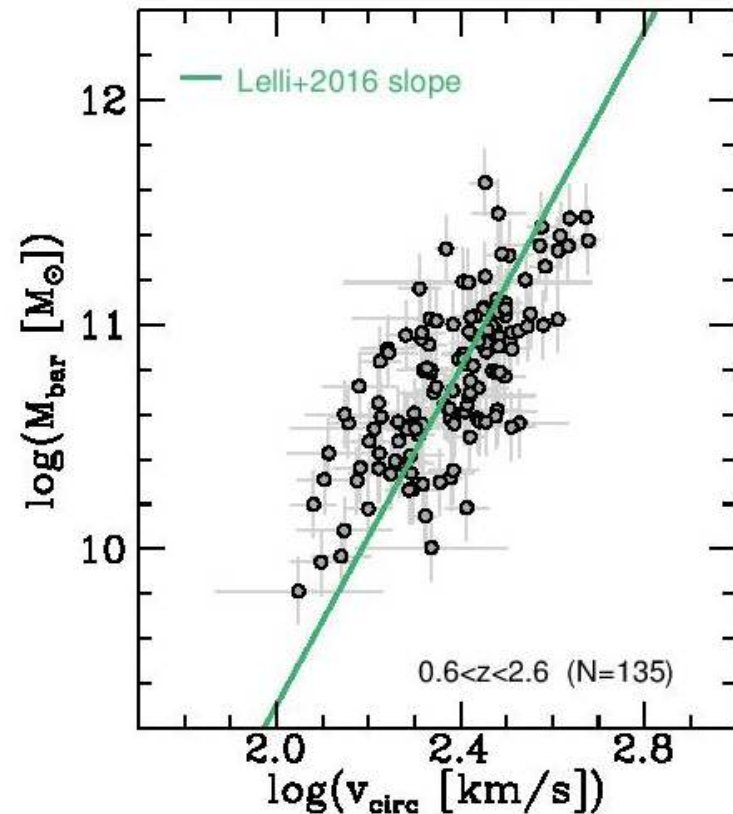
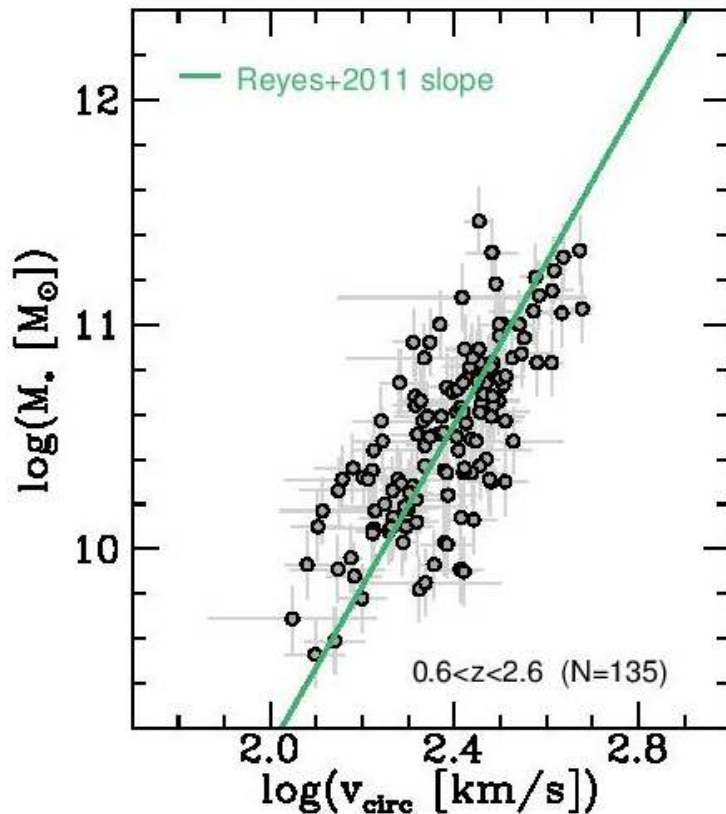
^aMS offset with respect to the broken power law relations derived by [Whitaker et al. \(2014\)](#), using the redshift-interpolated parametrization by [W15](#), $\Delta \text{MS} = \text{SFR} - \text{SFR}_{\text{MS}(z, M_*)[\text{W14}]}$.

^bOffset from the mass-size relation of SFGs with respect to the relation derived by [van der Wel et al. \(2014\)](#), $\Delta \text{M-R} = R_e^{5000} - R_{e, \text{M-R}(z, M_*)[\text{vdW14}]}^{5000}$, after correcting the *H*-band R_e to the rest-frame 5000 .

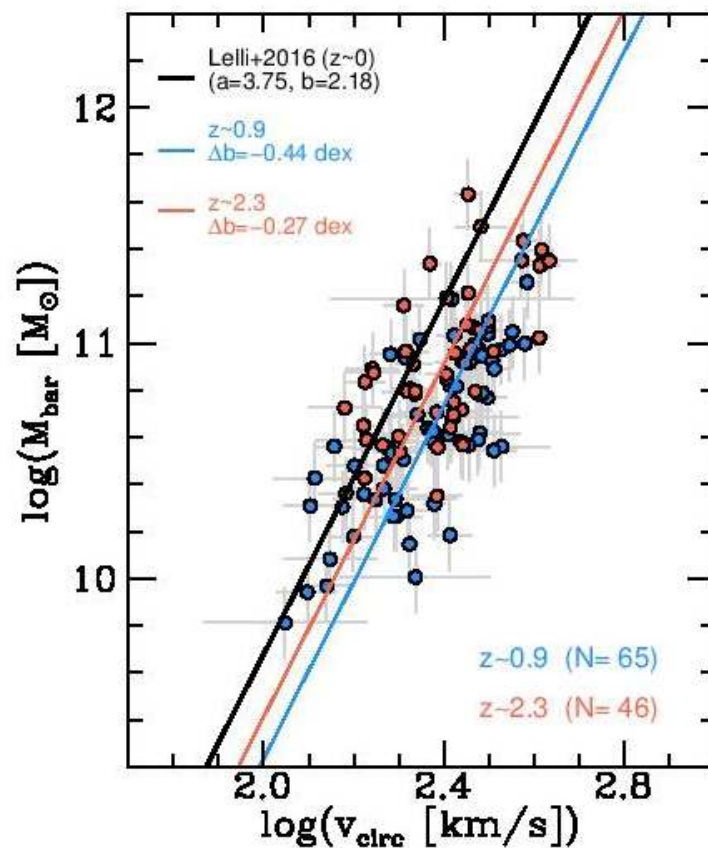
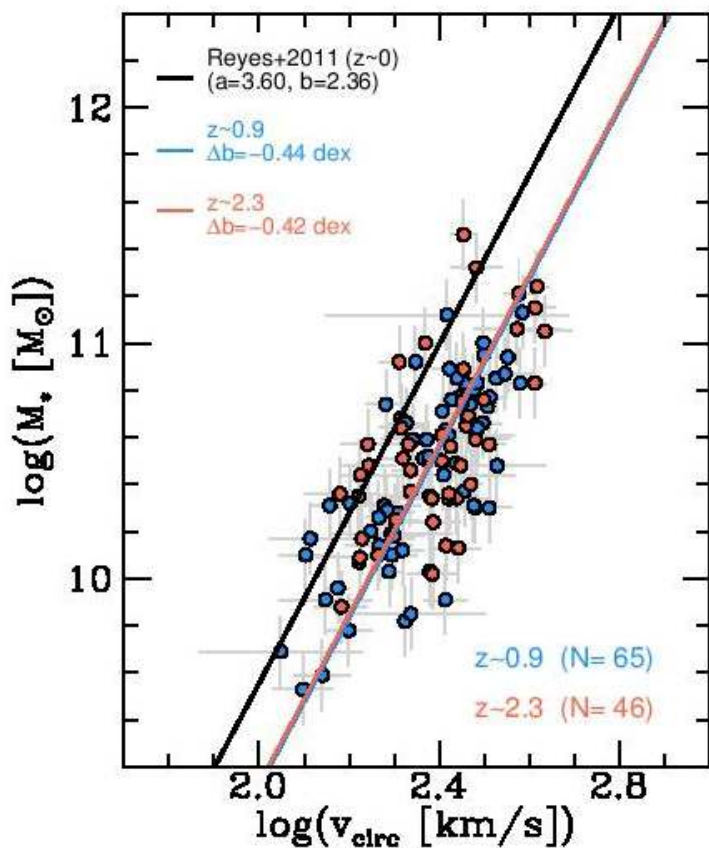
Измерения

- Напрямую измерялись только скорость вращения, звездная масса и SFR;
- А вот барионная масса...
- Количество газа оценивалось статистически по зависимости времени исчерпания газа от красного смещения, массы, отступления от главной последовательности и еще много чего... (Taccioni et al. 2017)

Суммарная Tully-Fisher



Tully-Fisher с разбиением по красному смещению

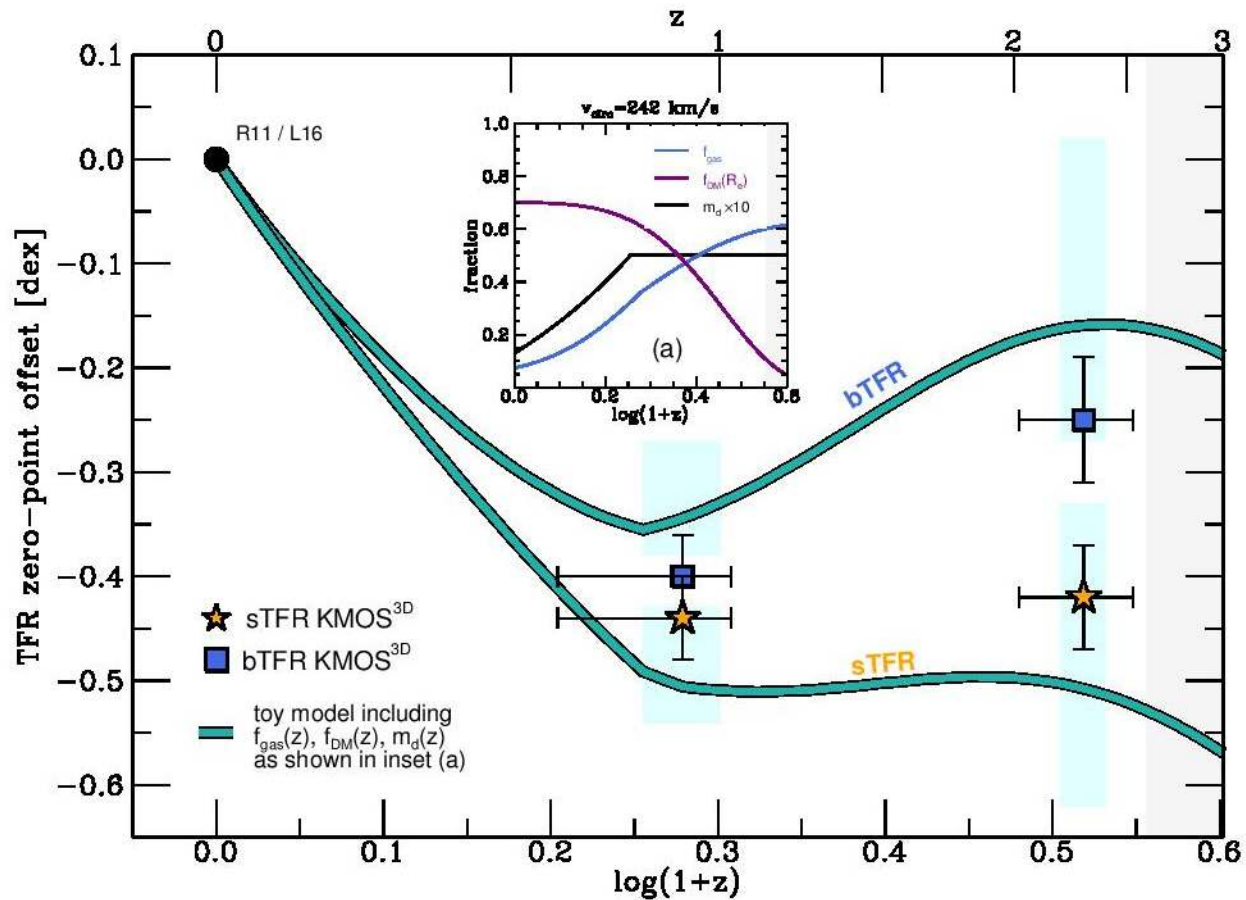


Измерения нуль-пункта

Table 2. Results from the inverse linear regression fits to Equation (4) using the least-squares method, including bootstrapped errors of the zero-point. The reference velocity is $v_{\text{ref}} = 242$ km/s.

TFR	redshift range	number of galaxies	slope a (local relation) $\left[\frac{\log(M [M_{\odot}])}{\log(v_{\text{circ}} [\text{km/s}])} \right]$	zero-point b (error) $[\log(M [M_{\odot}])]$	intrinsic scatter ζ_{int} $[\text{dex of } M_{\odot}]$
sTFR	$0.6 < z < 2.6$	135	3.60 (Reyes et al. 2011)	10.50 (± 0.03)	0.22
	$z \sim 0.9$	65	3.60 (Reyes et al. 2011)	10.49 (± 0.04)	0.21
	$z \sim 2.3$	46	3.60 (Reyes et al. 2011)	10.51 (± 0.05)	0.26
bTFR	$0.6 < z < 2.6$	135	3.75 (Lelli et al. 2016)	10.75 (± 0.03)	0.23
	$z \sim 0.9$	65	3.75 (Lelli et al. 2016)	10.68 (± 0.04)	0.22
	$z \sim 2.3$	46	3.75 (Lelli et al. 2016)	10.85 (± 0.05)	0.26

Вариации нуля-пункта с красным смещением



Astro-ph: 1703.05247

WISDOM Project – I: Black Hole Mass Measurement Using Molecular Gas Kinematics in NGC 3665

Kyoko Onishi,^{1,2*} Satoru Iguchi,^{1,2} Timothy A. Davis,³ Martin Bureau,⁴
Michele Cappellari,⁴ Marc Sarzi⁵ and Leo Blitz⁶

¹*Department of Astronomical Science, SOKENDAI (The Graduate University of Advanced Studies), Mitaka, Tokyo 181-8588, Japan*

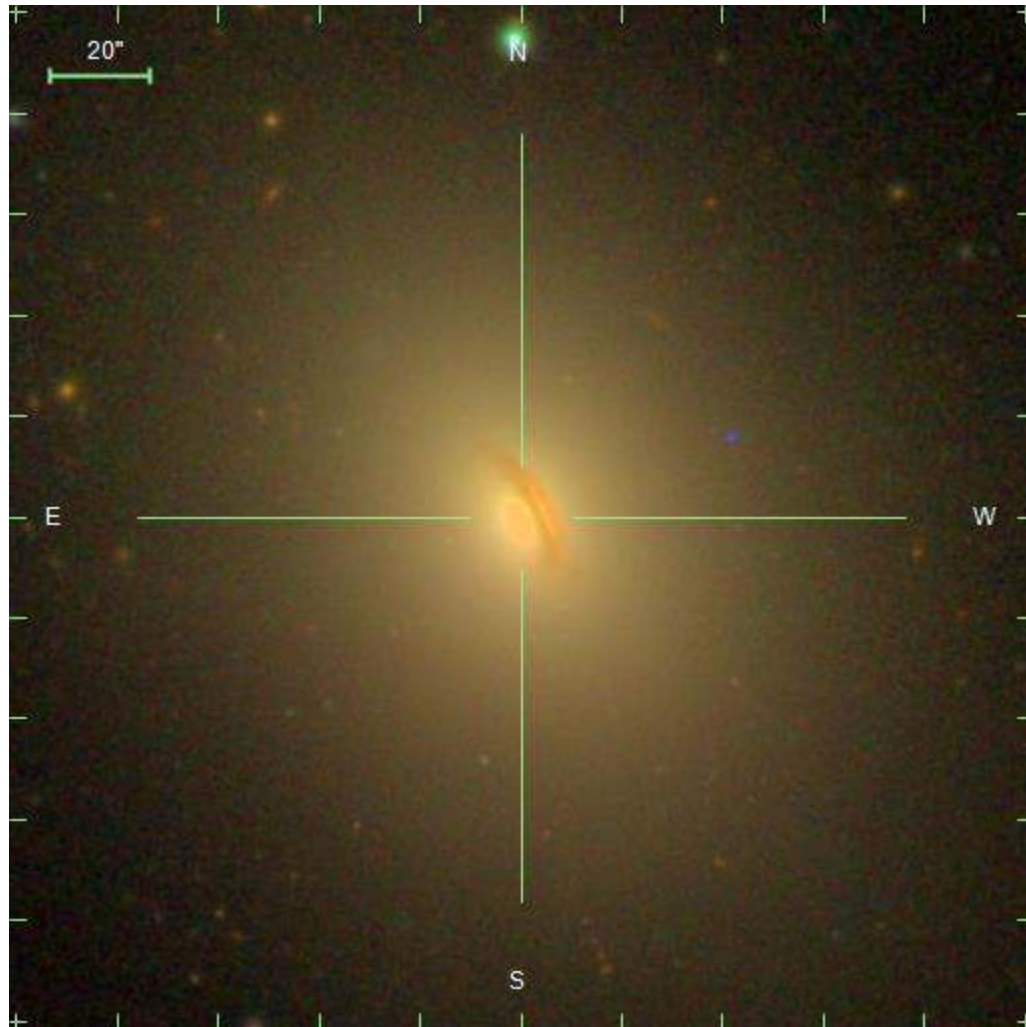
²*National Astronomical Observatory of Japan, Mitaka, Tokyo 181-8588, Japan*

³*School of Physics & Astronomy, Cardiff University, Queens Buildings, The Parade, Cardiff CF24 3AA, UK*

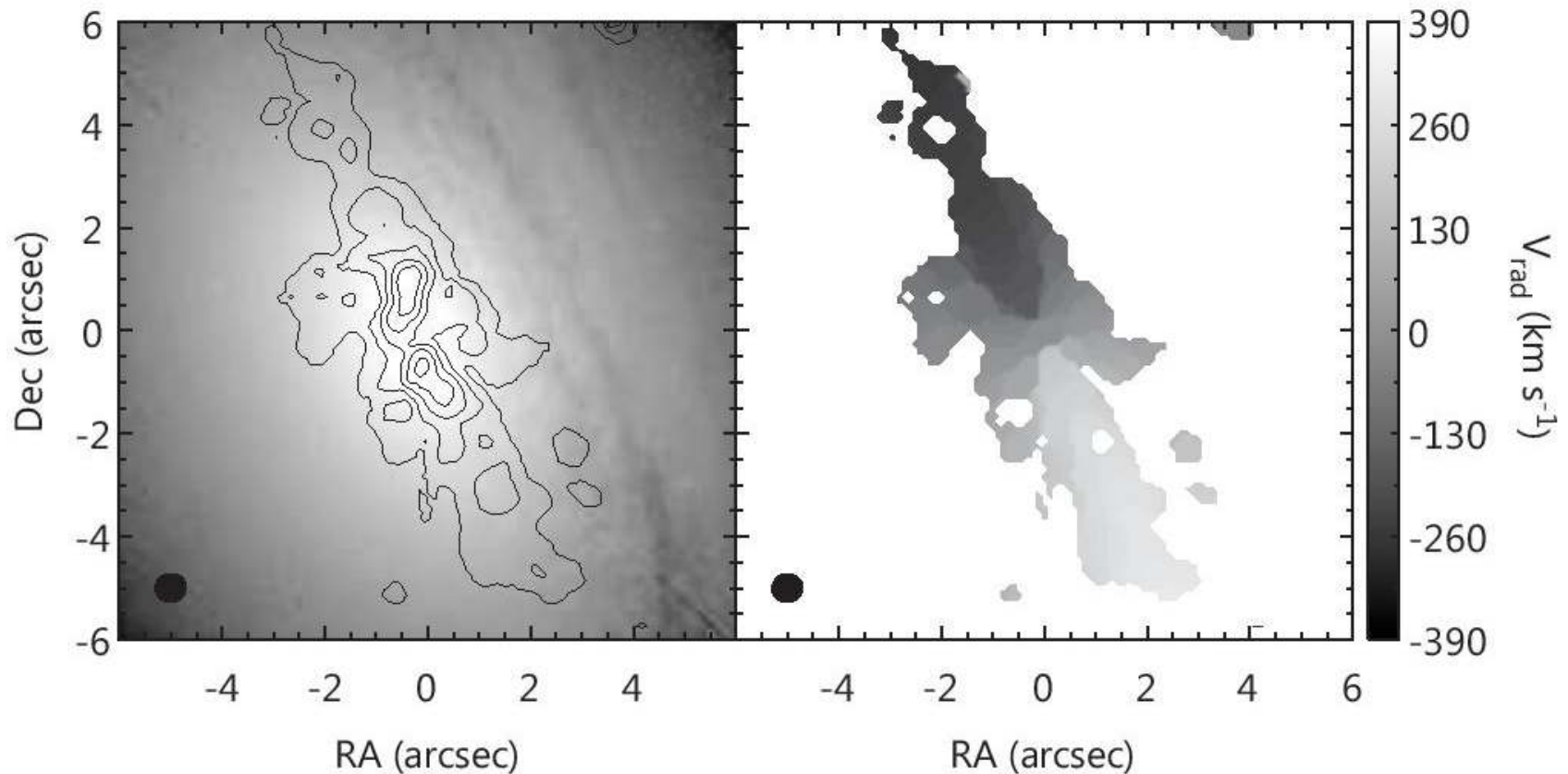
⁴*Sub-department of Astrophysics, Department of Physics, University of Oxford, Denys Wilkinson Building, Keble Road, Oxford OX1 3RH, UK*

⁵*Centre for Astrophysics Research, University of Hertfordshire, Hatfield, Herts AL1 9AB, UK*

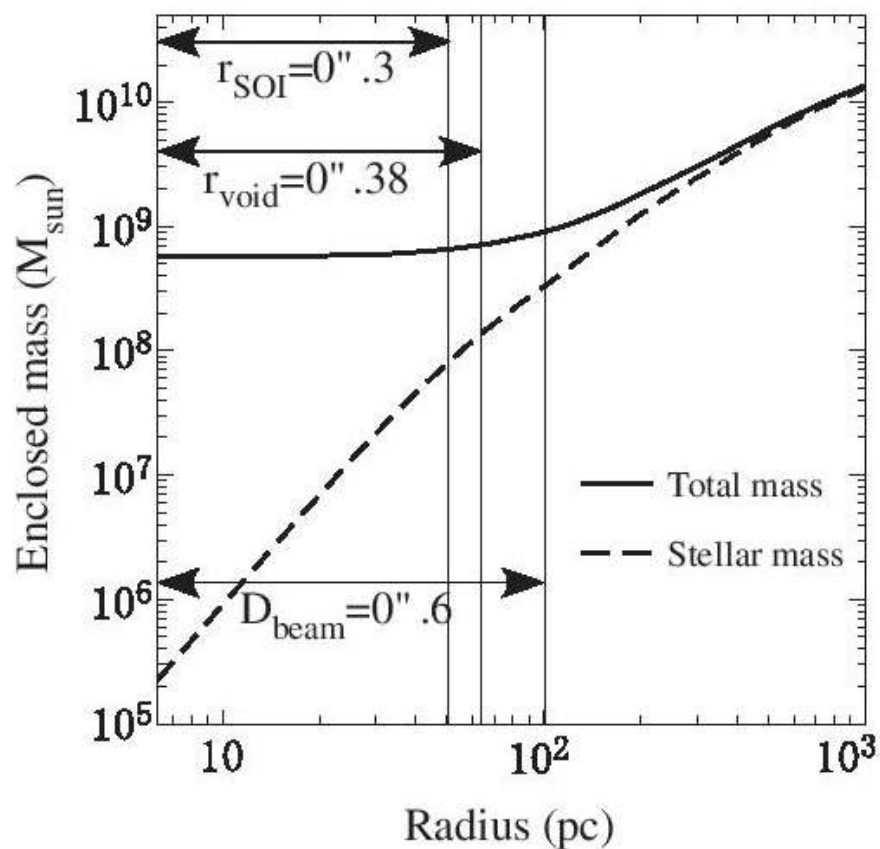
⁶*Department of Astronomy, University of California, Berkeley, California 94720, USA*



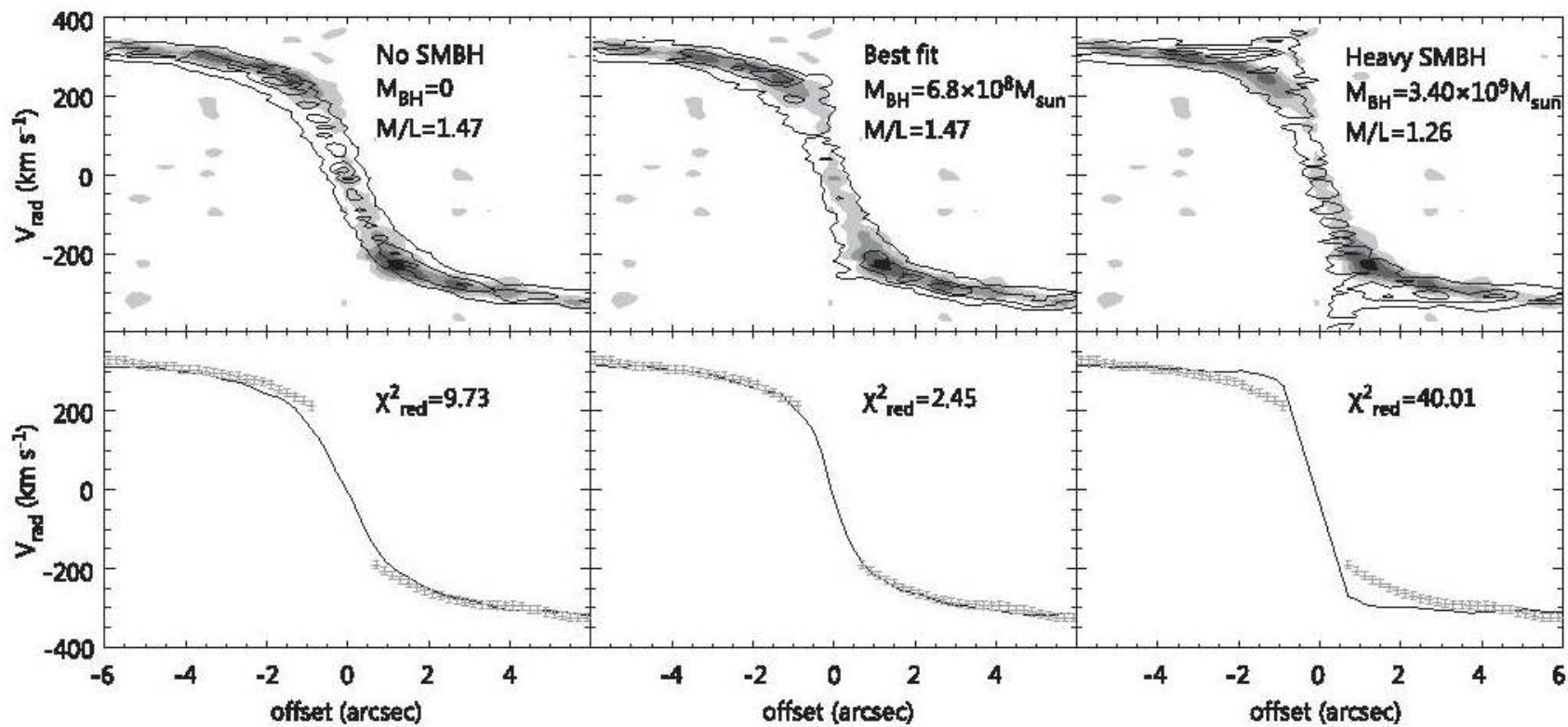
Центральный молекулярный газ



Двумерная модель поля скоростей дает...



P-V диаграмма дает то же самое



Astro-ph: 1703.05248

WISDOM Project – II: Molecular gas measurement of the supermassive black hole mass in NGC4697

Timothy A. Davis^{1*}, Martin Bureau², Kyoko Onishi^{3,4}, Michele Cappellari², Satoru Iguchi^{3,4}, and Marc Sarzi⁵

¹*School of Physics & Astronomy, Cardiff University, Queens Buildings, The Parade, Cardiff, CF24 3AA, UK*

²*Sub-department of Astrophysics, Department of Physics, University of Oxford, Denys Wilkinson Building, Keble Road, Oxford OX1 3RH, UK*

³*Department of Astronomical Science, SOKENDAI (The Graduate University of Advanced Studies), Mitaka, Tokyo 181-8588, Japan*

⁴*National Astronomical Observatory of Japan, Mitaka, Tokyo 181-8588, Japan*

⁵*Centre for Astrophysics Research, University of Hertfordshire, Hatfield, Hertfordshire, AL1 9AB, UK*

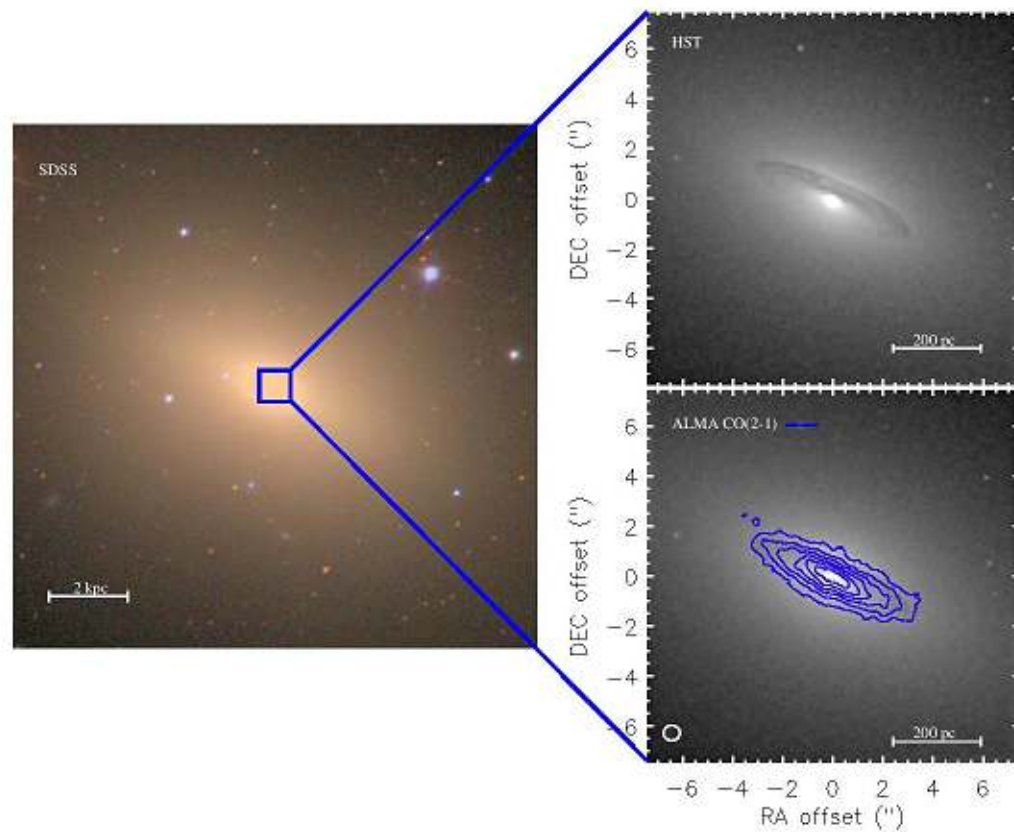


Figure 4. *Left panel:* SDSS three-colour (*grI*) image of NGC4697, $4' \times 4'$ ($13.2 \text{ kpc} \times 13.2 \text{ kpc}$) in size. *Right panel, top:* Unsharp-masked *HST* Advanced Camera for Surveys (ACS) F850LP image of a $825 \text{ pc} \times 825 \text{ pc}$ region (indicated in blue in the left panel) around the nucleus, revealing a clear central dust disc. *Right panel, bottom:* As above, but overlaid with blue $^{12}\text{CO}(2-1)$ integrated intensity contours from our ALMA observations. The synthesised beam ($0''.54 \times 0''.52$, $30^\circ \times 29^\circ$) is shown as a white ellipse in the bottom-left corner of the panel.

Двумерная модель поля скоростей молекулярного газа

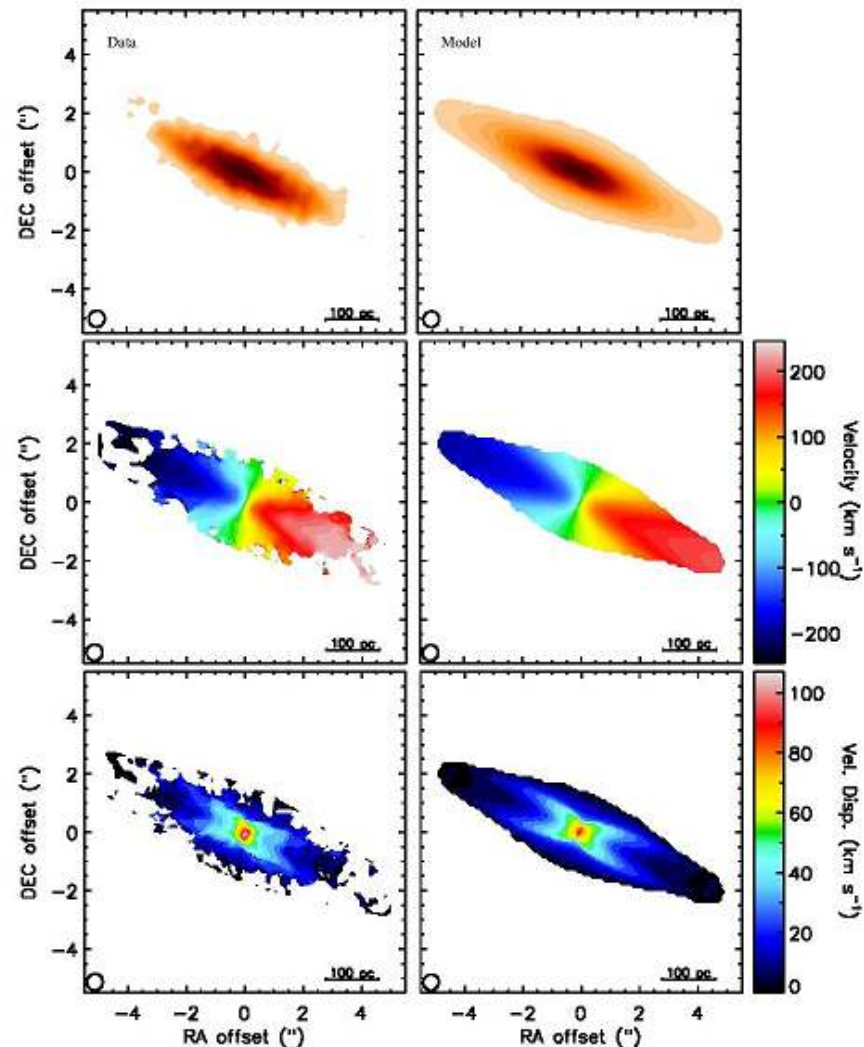


Figure 7. Integrated intensity, mean velocity and velocity dispersion maps of the $^{12}\text{CO}(2-1)$ emission in NGC4697. The moments extracted from the observations are shown in the left panels, while the same moments extracted in an identical way from our best-fit model are shown in the right panels.

P-V диаграмма вдоль большой оси

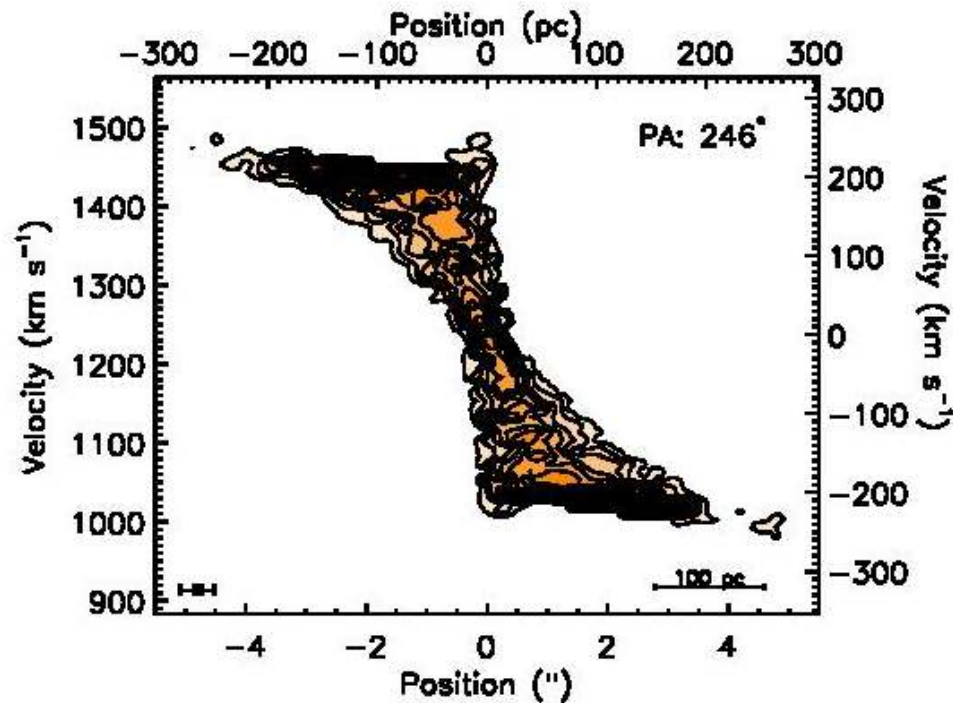


Figure 2. Position-velocity diagram of the $^{12}\text{CO}(2-1)$ emission in NGC4697, extracted along the kinematic major axis. The synthesised beam size (along the major axis) and spectral resolution of our observations is indicated as an error bar in the bottom-left corner. A steep increase of the

Модель с черной дырой (130 млн солнечных масс)

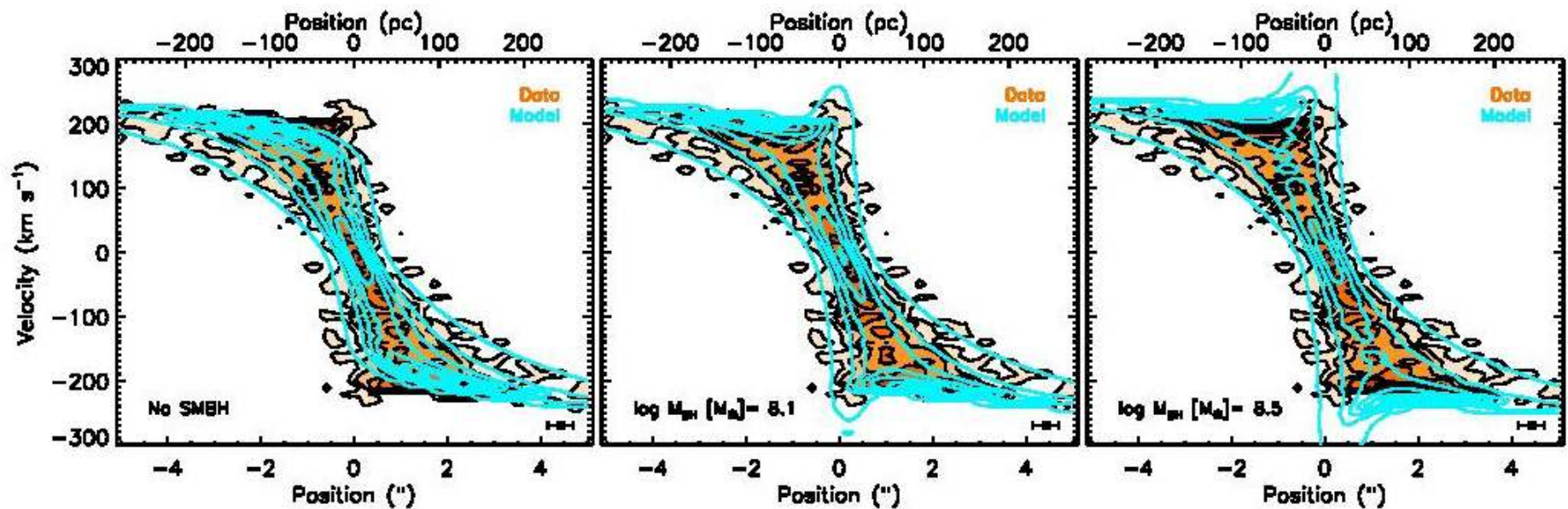


Figure 8. As Figure 2, but overlaid with model PVDs extracted in an identical fashion from models that only differ by the central SMBH mass (blue contours). The left panel has no SMBH, the centre panel shows our best-fit SMBH mass, and the right panel has an overly massive SMBH. The legend of each panel indicates the exact SMBH mass used. A model with no SMBH is clearly not a good fit to the data.

Место в общей статистике

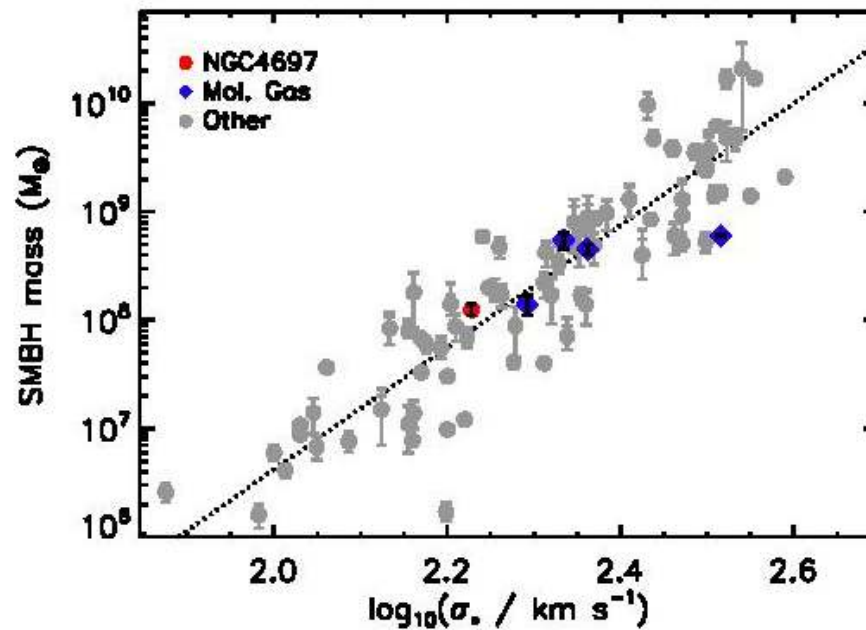


Figure 10. $M_{\text{BH}} - \sigma_*$ relation from the compilation of McConnell & Ma (2013) (grey points and dotted line). We also show the SMBH mass measured for NGC4697 in this paper as a red circle and highlight measurements from other works also using the molecular gas technique with blue diamonds.

Astro-ph: 1703.05610

LETTER TO THE EDITOR

The HI content of isolated ultra-diffuse galaxies: a sign of multiple formation mechanisms?

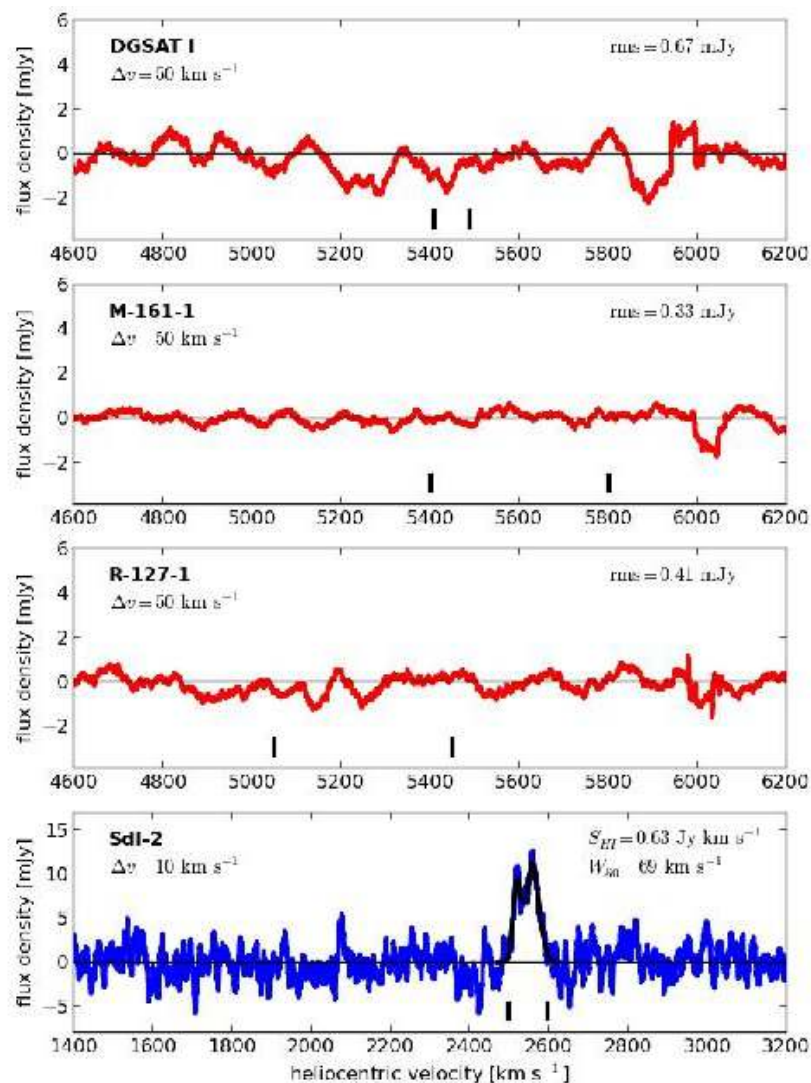
E. Papastergis^{1,*}, E.A.K. Adams² and A.J. Romanowsky³

¹ Kapteyn Astronomical Institute, University of Groningen, Landleven 12, Groningen NL-9747AD, The Netherlands
e-mail: papastergis@astro.rug.nl

² ASTRON, the Netherlands Institute for Radio Astronomy, Postbus 2, Dwingeloo NL-7900AA, The Netherlands
e-mail: adams@astron.nl

³ Department of Physics & Astronomy, San José State University, One Washington Square, San Jose, CA 95192, USA
e-mail: aaron.romanowsky@sjsu.edu

Из 4х галактик увидели газ (21см) ТОЛЬКО В ОДНОЙ



Место в общей статистике – разное происхождение ультрадиффузных галактик

